# An approach to evaluate the wear of customized manufacturing fixtures through the analysis of 3D scan data

Materials Today: Proceedings xxx (xxxx) xxx

Contents lists available at ScienceDirect

Materials Today: Proceedings

journal homepage: www.elsevier.com/locate/matpr

# An approach to evaluate the wear of customized manufacturing fixtures through the analysis of 3D scan data

Mankirat Singh Khandpur *, Paolo Minetola, Vito Stiuso, Serena Rifuggiato, Luca Fontana, Erika Lannunziata, Alberto Giubilini, Luca Iuliano

*Politecnico di Torino, Department of Management and Production Engineering (DIGEP), Corso Duca degli Abruzzi 24, 10129 Torino, Italy*

ARTICLE INFO

*Article history:*
Available online xxxx

*Keywords:*
Wear
3D scanning
Additive manufacturing
Fixtures
Alumide

ABSTRACT

With the recent gain in popularity and adoption of additive manufacturing in various industrial sectors, quality assessments to determine the functionality of 3D printed parts are critical. This holds especially when the parts are subjected to wear as in the case of the production of customized fixtures. Some reinforced polymeric materials for additive manufacturing can be employed as a substitute for low-resistance metals like Aluminium. In this paper, a custom-made tribometer was used to simulate the wear of 3D printed fixtures of Alumide material for sheet metal inspection operations. Contact 3D scanning is used to monitor the condition of the fixture for increasing numbers of wear cycles. This study aims to calculate the wear volume of cylindrical pins starting from the surface points of 3D scan data. The methodology employs alpha shapes to obtain the progression of the volume and area of the worn zone. Experimental tests to evaluate the wear volume were carried out to compare the durability of Alumide to that of Aluminium, filling the gap of previous literature, which had focused exclusively on diametral wear. The findings indicate a better wear resistance for Alumide specimens and this work contributes to broadening the knowledge about the wear behaviour and the lifetime of 3D printed parts.

Selection and peer-review under responsibility of the scientific committee of the Fourth International Conference on Recent Advances in Materials and Manufacturing 2022.

## 1. Introduction

Fixtures are an important element to achieve high-quality levels in manufacturing. Fixtures are used to locate and hold securely in position a single part or a subassembly during different operations along the manufacturing route. It was estimated that dimensioning errors, attributed to inadequate fixture design, can account for about 40% of rejected parts [1]. Therefore, low-quality fixturing systems can have a direct and negative effect on the output quality and cost-effectiveness of a production system. In this regard, the use of additive manufacturing (AM) technologies in the fabrication of custom fixtures enabled a significant advancement in the industrial field [2]. Among all its advantages, the use of AM in fixture fabrication enables great freedom from any geometric constraint, as well as a reduced production time with a shorter supply chain [3–6]. Among AM technologies, selective laser sintering (SLS) and Continuous Fiber Fabrication (CFF) are two consolidated processes for layerwise manufacturing of durable fixtures of composite materials. The former process can be applied for the production of fixtures made of Alumide material by layerwise melting polyamide 12 powders containing Aluminium particles [7]. The latter process, which is patented by Markforged company, can be used for the fabrication of fixtures by extrusion of Onyx, a polyamide filament containing carbon particles, with the possibility of increased reinforcement by continuous carbon fibres [8,9]. As an alternative to Markforged Onyx material, traditional 3D printing of Fused Filament Fabrication (FFF) of a filament reinforced with carbon particles can also be employed [10].

One of the first software packages for rapid tooling (RT) of custom fixtures devices was the pioneer design module RapidFit of Magics software by Materialise [7]. Nevertheless in their recent work [11], Gameros et al. reviewed some of the most interesting fixturing designs and simulations and commented their implementation within the production systems. For example, Selective Laser Sintering (SLS) was used to build custom fixtures to hold intricate

* Corresponding author.
*E-mail address:* mankirat.khandpur@polito.it (M.S. Khandpur).

https://doi.org/10.1016/j.matpr.2023.03.385
2214-7853/
Selection and peer-review under responsibility of the scientific committee of the Fourth International Conference on Recent Advances in Materials and Manufacturing 2022.

geometries during a grinding process. In addition, some more recent case studies of 3D printed fixtures were considered to hold different parts during automated 3D scanning [12,13].

All these technologies and related materials can be used for metal replacement in the fabrication of durable customized fixtures for manufacturing operations. However, the durability of 3D printed composites differs from the one of metals [14]. In fact, because of friction, fixtures suffer wear during loading and unloading of parts and, after a certain time, custom AM elements must be replaced. To date, only a limited number of studies were conducted to investigate the wear behaviour of 3D printed fixtures. To assess the durability of customized AM fixtures, the authors have designed a specific tribometer named reverse guillotine [15,16]. This apparatus, comprising a motorized linear platform, can be used to simulate the wear that is caused by the sliding of a sheet metal part on the fixture material during mounting and unmounting operations.

This work aims to evaluate the volume wear of a customized AM fixture through repeated sliding cycles simulating these operations. The diametral wear of the AM fixture was evaluated in a previous work [16] by measuring the size reduction of some pin diameters using a coordinate measuring machine (CMM). In this research, 3D scan data of the pin surface were used to calculate the volume of worn fixtures, tested on the reverse guillotine tribometer. Then, automatic routines in Matlab were designed and implemented to calculate the volume of material loss during the sliding action as well as the volume of material that was subjected to plastic deformation on the pin surface. This approach was applied to both Alumide and Aluminium samples for comparing and discussing the results for the two materials through two different wear indicators, i.e diametral and volume wear. Thus, the novelty of this research relies on the development of a more in-depth understanding of the fixture wear assessment, introducing a new approach for calculating the wear volume from 3D scan data.

## 2. Materials and methods

### 2.1. Test samples

The geometry of the test specimen is shown in Fig. 1. The sample has a square base of 40 mm side with 10 mm thickness. The base has four holes that are used to locate and hold the sample into position on the wear testing machine and the 3D scanning device. A cylinder with a 16 mm diameter and 20 mm height is used to connect the active part of the sample to the base. The active part of the sample, which undergoes wearing, is a cylindrical pin of 8 mm diameter with 20 mm height.

To compare the resistance to wear of Alumide material to the one of Aluminium, one replica of the specimen was produced for each material.

The Alumide sample was produced using the SLS process with the building direction of layer addiction coinciding with the pin axis, i.e. from the base to the small pin. The specimen was fabricated using a P395 EOS machine and adopting a layer thickness of 150 μm as suggested in the EOS material data sheet.

The Aluminum specimen was made of AA2024 alloy by machining a square block on a numerical controlled 3-axis milling machine.

Before starting the wear test, each specimen was scanned to acquire the condition of the sound unworn surface of the pin in the as-built surface resulting from the manufacturing process. The initial scan data of the pin were referred to as 0 cycle data and were used as a reference for the evaluation of wear progression. The as-built specimen was scanned as detailed in the next section 2.3.

### 2.2. Wear test

The custom-made tribometer for the wear test was built using a commercial Limes 122 motorized positioning system by OWIS. The step motor of the OWIS system was used to move the test specimen relatively to the sheet metal part. As the specimen is mounted on an L-shaped support connected to the carriage of the OWIS system, the pin axis is horizontal. Therefore, to keep the hole of the sheet metal in contact with the pin during the wear test, a vertical reverse guillotine connected to a pre-loaded spring was used (Fig. 2).

The wear test was carried out by applying a horizontal alternating motion to the 8 mm pin with the OWIS carriage. The worn area (Fig. 1) is centred on the pin length and for every wear cycle the carriage moves 10 mm forward and 10 mm backwards with a speed of 0.60 m/min. During the cycles, the sheet metal is pulled upward by the spring of the vertical guillotine to contact the specimen pin (Fig. 3).

Considering the material resistance to wear and abrasion, the test was stopped every 250 cycles for the Alumide specimen and every 500 cycles for the Aluminium sample. The interruption of the test was used to monitor the state of the pin surface and dimensionally inspect the pin area in contact with the sheet metal. For this purpose, the specimen was unmounted from the support on the carriage of the OWIS system and was moved to the 3D scanning device for the inspection operations. After dimensional measurements, the sample was placed back on the OWIS carriage, and the test was repeated until the next interruption.

The test was finally stopped when the average diametral wear of the pin exceeded 0.10 mm. This reduction of the diameter was assumed as the limit for the wear test since it might jeopardize fixture functionality. Such a clearance between the hole in the sheet metal and the pin diameter might introduce systematic errors in part positioning and negatively affect the results of part inspection.

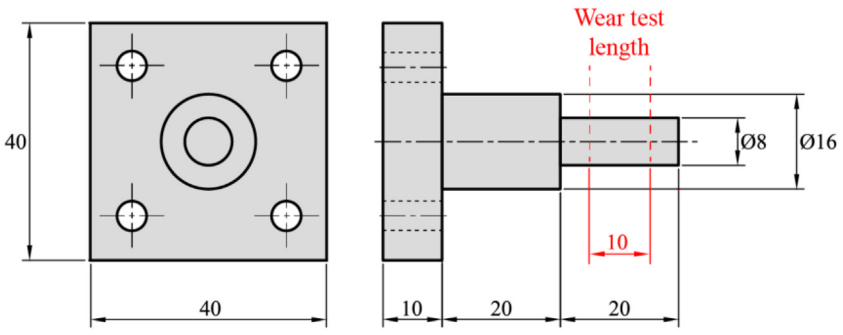


**Fig. 1.** Specimen geometry for the wear test of fixtures.

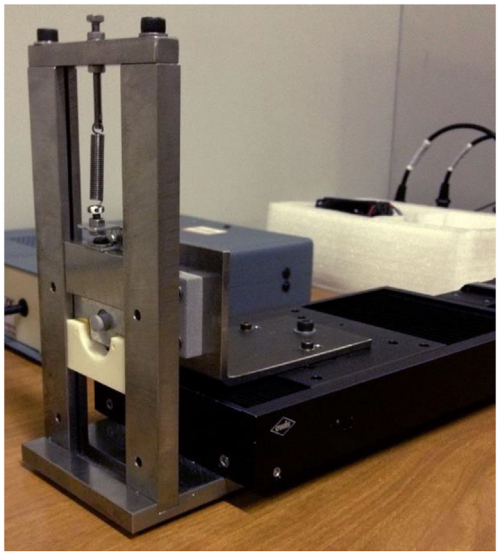

**Fig. 2.** Wear test tribometer with the Alumide specimen.

**Fig. 3.** Detail of the contact area between the AA2024 specimen and the sheet metal during the wear test.

### 2.3. 3D scanning

Before reaching the wear limit, at each interruption of the test, the worn area of the specimen was digitized using a Picza Pix-4 digitizer by Roland (Fig. 4a). The Picza device is a piezoelectric 3D scanner that uses a metal needle to inspect the surface of the digitized object and transfer the X, Y and Z coordinates of the contact point to a PC with Dr. Picza software. The origin of the reference frame is located in the bottom left corner of the machine platform (Fig. 4a). The X axis is aligned to the length of the platform, while the Y axis is aligned to its width. The Z axis is pointing upward and has the origin located on the platform plane (XY plane).

The Pix-4 model has a working area of 152.4 mm (X direction) × 101.6 mm (Y direction). The maximum scan height is 60.5 mm (Z direction). The needle-shaped probe has a length of 64 mm with a tip bulb diameter of 0.08 mm (Fig. 4b). The maximum scan resolution is 0.05 mm in the X and Y directions, while it is increased by 50% (0.025 mm) in the Z direction. The scan speed is 30 mm/s in the X and Y directions and 9 mm/s in the Z direction.

Once the scan area is defined by the user in Dr. Picza, the Picza scanner works automatically and acquires the coordinates of the surface points, creating a 3D point cloud with a regular grid, whose density depends on the resolution set for the X, Y and Z axes. The specimen was mounted on the Picza device with the main axis of the cylindrical shapes parallel to the scanner platform, as shown in Fig. 4b. The worn surface was oriented upwards pointing at the touch probe. To fully include the worn surface of the pin, for the Alumide and Aluminium specimens the scan was set with a length of about 25 mm in the X direction and 12 mm in the Y direction (Fig. 5a). That area was scanned at the maximum resolution of the Picza device in about 8 h at every wear test interruption for specimen monitoring. The supporting cylinder of 16 mm in diameter was partially included in the scan area to have a reference for subsequent alignment operations that were applied for wear estimation and comparison with the reference unworn pin surface at 0 wear cycles. An example of the results of contact digitizing of the worn specimen surface is shown in Fig. 5b for the Aluminium specimen at 4500 cycles. In this figure, the pin surface is represented as a tessellated 3D mesh of triangles that are automatically generated in Dr. Picza software by connecting the nearest points in the point cloud. The grid of points and mesh has a resolution of 0.05 mm in both X and Y directions.

## 3. Data analysis

### 3.1. Alignment of 3D scan data

After 3D scanning, the tessellated point cloud was exported from Dr. Picza software to the standard STL format. The STL files corresponding to a different number of wearing cycles were then imported into GOM Inspect software. GOM Inspect is a commercial software by the German company GOM GmbH (recently acquired by Carl Zeiss AG metrology group) for dimensional inspection of

a b

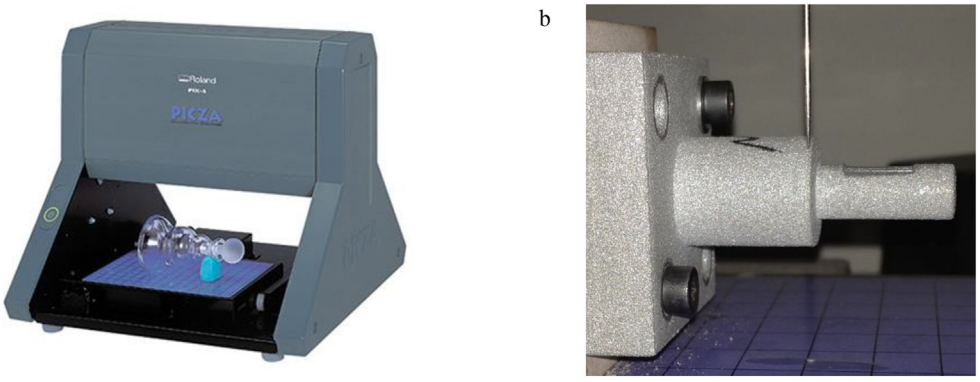


**Fig. 4.** Picza Pix-4 piezoelectric contact 3D scanning device (a); digitizing of the Alumide specimen (b).

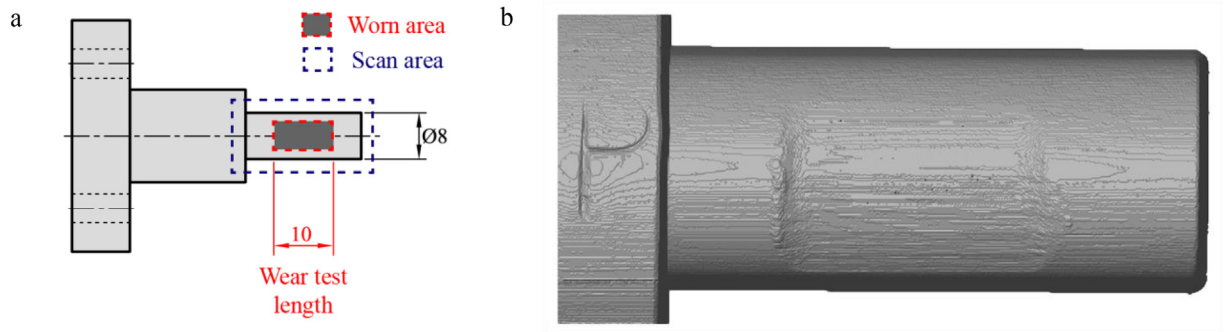


**Fig. 5.** Top view of the worn area of the pin with the indication of the 3D scan area for the Picza Pix-4 digitizer (a); result of the 3D scanning for the Alumium specimen at 4500 cycles (b).

parts from their 3D scan data [17]. At each wear test interruption, GOM software was used to align the scan data with the reference data of the unworn pin at the initial condition of 0 cycles (Fig. 6). The alignment was carried out using the pre-alignment function of GOM Inspect that is based on a best fitting algorithm, i.e. a least square method that allows minimizing the distance between corresponding points of the compared point clouds.

All aligned scan data to the 0-cycle reference was then exported again from GOM Inspect software as STL files without modification of the initial points and triangular mesh structure. All aligned STL models were then imported into Matlab software by Mathworks, where specific algorithms were developed to calculate volumes from the pin surface data.

### 3.2. Identification of worn area

After importing the aligned scan data of the specimens in Matlab, the set of points was reduced to speed up computational times as it is not useful and convenient to consider points belonging to the specimen surface in those areas that were not altered by the wear test.

Because of the scanning configuration (Fig. 4b), only the top half of the pin was scanned as the limit points for the contact of the needle with the cylindrical shapes are the diametral points of the top half of each cylinder. When the needle was in contact with these points, the specimen shape had a vertical tangent. Thus, vertical surfaces were created by Dr. Picza software in the Z direction (Fig. 6). To exclude these faces from all scans, the points below a common Z level, which was lower than the pin diameter, were deleted in Matlab. In the remaining data set, the points to be considered were further reduced by cropping a rectangular area of about 14 mm in the X direction and 10 mm in the Y direction including the worn zone and its surroundings (Fig. 7).

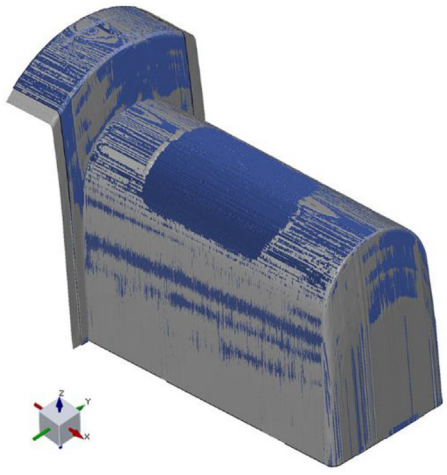

**Fig. 6.** Alignment of the Aluminium scan data at 4500 cycles with the reference data of the unworn specimen at 0 cycles.

A tessellated representation of the two datasets overlapping on the same figure using Matlab function "trimesh" is shown in Fig. 8a for visualization purposes only. In this figure, the black triangles are the reference data (Ref) of the pin at 0 cycles, while the red mesh elements represent the compared data (Comp) of the worn pin surface after a certain number of cycles.

These two datasets of 3D points were used to create their respective shapes by using the alpha shape function. By this function, a closed 3D bounding volume for each pointset was generated using a triangular mesh. The 3D shape was created considering an alpha disk or sphere over the points. If the alpha radius is set to default, the function automatically finds the minimum radius for the tightest fitting of the pointset. The 3D shapes of the Ref data and Comp data were used to identify their relative complementary regions with respect to each other. These regions of the specimen correspond to two different types of material alteration of the pin surface. The former region (Fig. 8b) can be distinguished by the presence of Ref data points that lay over the Comp data points. This region corresponds to the area where wear takes place, and the specimen material was deformed and removed by the abrasion action of the sliding sheet metal. The latter region (Fig. 8c) is located near the borders of the wear test area in the sliding direction. The motion of the sheet metal and the abrasion action pushed a small amount of material outside the worn area near its borders, where the sliding motion is inverted at the extremes of the 10 mm test length. Hence, this procedure aims to calculate the wear volume for the first region and the volume of the additional material in the second region because of the plastic deformation. Hereafter, we will refer to the subtracted material (Fig. 8b) as positive wear and to the additional material (Fig. 8c) as negative wear.

Moreover, local wear can be displayed as a colour map (Fig. 9) on the pin surface by associating the 3D pointset of Comp data with the colours that represent the difference in the Z coordinate of the Ref data to the Comp data. By assigning the dark red colour to the extreme positive value of the Z difference and the dark blue colour to the extreme negative difference, the area of positive wear (Fig. 8a) in the centre of the pin appears in red and those of negative wear (Fig. 8b) on the test zone border appear in blue in Fig. 9.

For the positive wear area, all the points of Ref data that lie outside the alpha shape of the Comp data were identified and their nearest neighbouring point belonging to the Comp data was searched. If the distance between two corresponding points is larger than 0.1 mm in the Z direction, these points were identified as

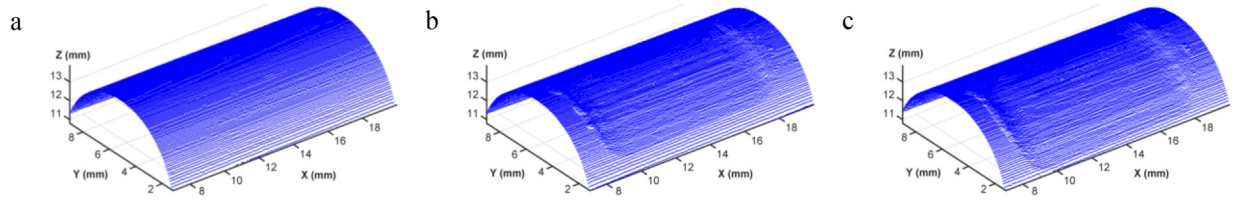


**Fig. 7.** 3D aligned and cropped scan data for the Aluminium specimen at 0 cycles (a), at 3000 cycles (b), and at 4500 cycles (c).

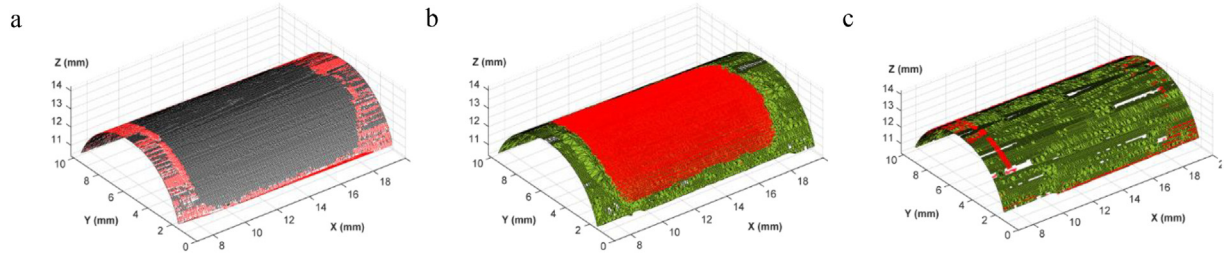


**Fig. 8.** Overlapped datapoints of Ref data against Comp data (a); points and region of positive wear for Comp data (b) and points and regions of negative wear for Comp data (c).

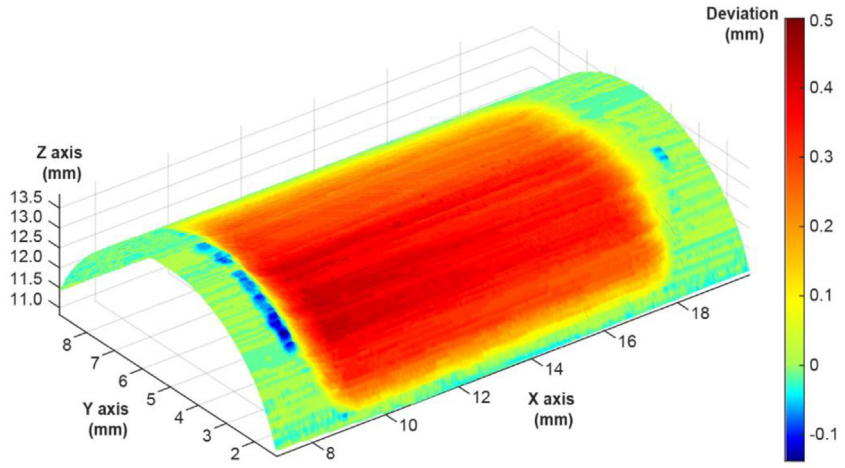


**Fig. 9.** Pin surface representation with colours representing the difference in the Z coordinate of Ref data compared to Comp data.

wear points, as highlighted in red colour in Fig. 8b. The value of the minimum distance of 0.1 mm was set as twice the maximum resolution of the Picza machine, in order to consider that unworn surfaces can have overlapping points within a tolerance equal to the scanning error.

For the negative wear areas, a similar methodology was used but considering all points of the Comp data which lie outside the Ref data. Whereas, as a threshold for the identification of homologous points belonging to the same unworn surface, the 0.1 mm distance was still considered. The resulting points in negative wear areas are shown in red colour in Fig. 8c.

### 3.3. Computation of volumes

After separating and categorizing the points belonging to the negative and positive wear areas, alpha shapes were generated once again to extract the volume of the two pointsets. Starting from the data in Fig. 8b, the positive wear shape in Fig. 10a was obtained, while the resulting negative wear shape is shown in Fig. 10b.

This result was achieved by first assigning the value of 0.25 mm to the alpha radius to create small islands in case of small groups of isolated neighbouring points, like those in the negative wear areas (Fig. 8c). Then the final 3D shape (Fig. 10b) was generated by setting the alpha radius to 0.4 mm.

Every 3D shape has a volume and a surface area. Although the surface extension of a 3D shape might seem large, the associated volume could be small if the difference in the Z level of the Comp data to the Ref data is small, due to a smaller material difference. Negligible volumes provide a small contribution to the total volume and wear estimation.

The maximum volumes were calculated for the positive and negative areas respectively. For the remaining volumes of each type of wear, only those whose value fitted within one tenth of the maximum volume were considered. All other smaller volumes were assumed as negligible and discarded. The final volumes are shown in Fig. 11a for the positive wear area and in Fig. 11b for the negative wear areas.

The extension of these volumes in the top view of the pin can also be traced by creating their tightest boundary in the XY plane. Fig. 12a shows the boundary with red colour for the points belong-

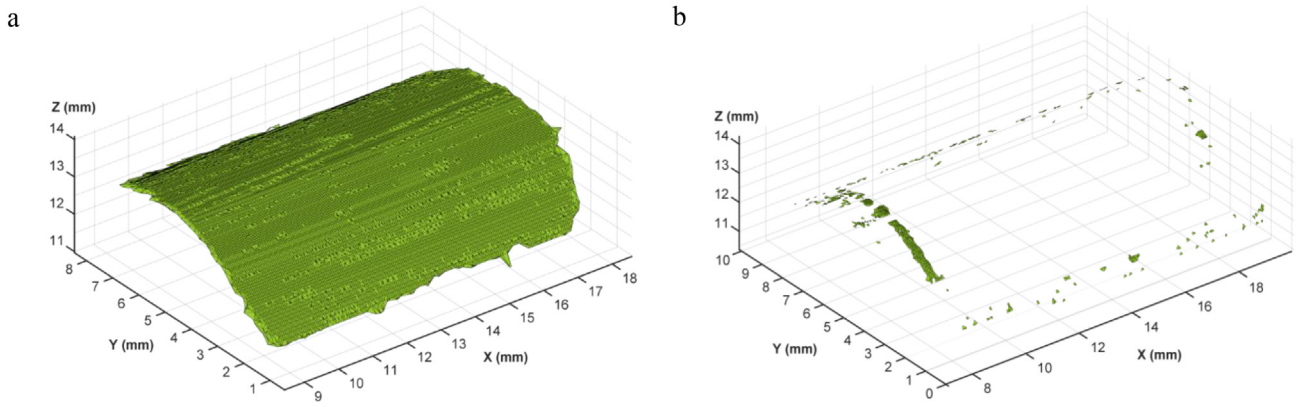


**Fig. 10.** Positive wear shape (a) and negative wear shape (b) including negligible volumes for Comp data.

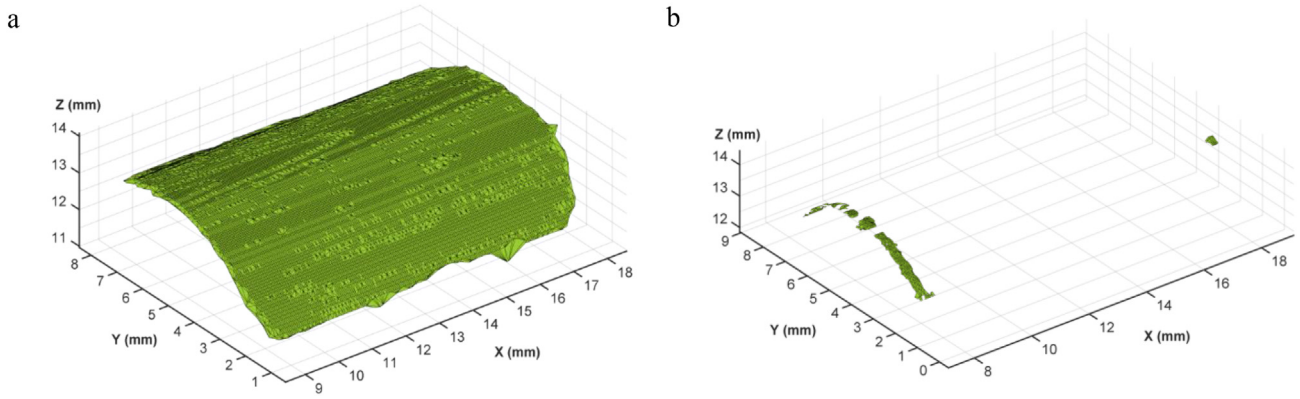


**Fig. 11.** Positive wear volume (a) and negative wear volume (b) without negligible volumes for Comp data.

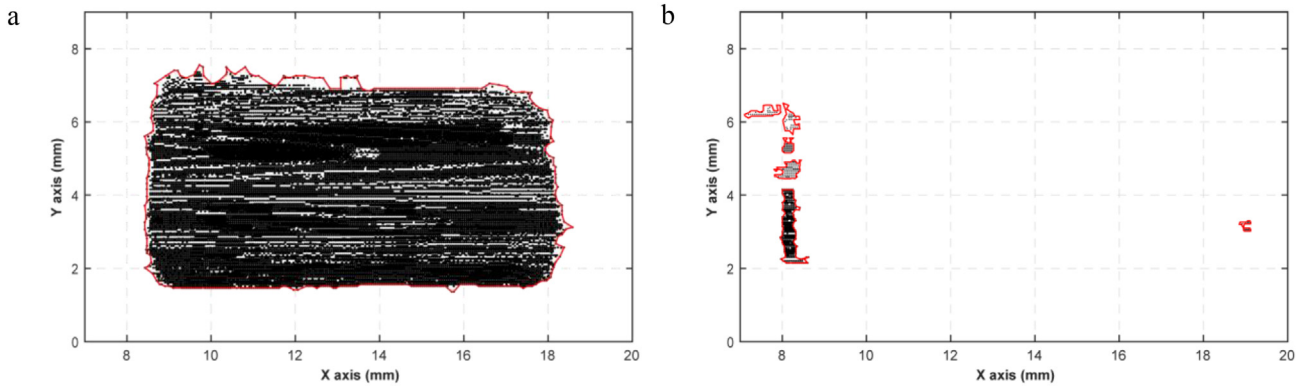


**Fig. 12.** Positive wear area (a) and negative wear areas (b) with highlighted boundaries for Comp data without negligible volumes.

ing to the positive wear area, whereas the boundaries of the volumes of additional material in the negative wear areas are traced in red in Fig. 12b.

## 4. Results

Following the methodology described in the previous section, the resulting wear volumes and the extension of the wear areas were calculated for the Alumide and the Aluminium specimens until the limit of 0.10 mm for the diametral wear of the pin was reached according to previous results [16].

The results for the Alumide sample are summarized in Table 1. As the number of wear cycles increases, an increasing trend in both the volume (Table 1) and area (Fig. 13) can be observed for the positive wear regions, whereas the development of negative wear regions is random.

Because of the alternating motion and contact of the sheet metal part on the pin at every new wear cycle, the specimen material underwent progressive abrasion in the wear zone. Starting from the ideal contact point of the hole in the sheet metal with the side wall of the cylindrical face of the pin, the area and volume of the worn material both increase. However, not all the material in the wear test zone was removed by the abrasion, but some fraction

**Table 1**
Wear volumes of Comp data for the Alumide test sample at different wearing cycles.

| Wear cycles | Positive wear volume ($mm^3$) | Negative wear volume ($mm^3$) |
|---|---|---|
| **500** | 2.24 | 0.03 |
| **1000** | 4.15 | 0.02 |
| **1500** | 6.56 | 0.04 |
| **2000** | 8.53 | 0.04 |
| **2500** | 10.49 | 0.02 |
| **3000** | 11.34 | 0.03 |
| **3500** | 11.37 | 0.04 |
| **4000** | 11.67 | 0.03 |
| **4500** | 11.77 | 0.03 |
| **5000** | 12.64 | 0.01 |
| **5500** | 13.56 | 0.05 |
| **6000** | 14.66 | 0.05 |

**Table 2**
Wear volumes of Comp data for the Aluminium test sample at different wearing cycles.

| Wear cycles | Positive wear volume ($mm^3$) | Negative wear volume ($mm^3$) |
|---|---|---|
| **500** | 1.55 | 0.08 |
| **1000** | 4.61 | 0.05 |
| **1500** | 7.54 | 0.05 |
| **2000** | 10.06 | 0.14 |
| **2500** | 12.32 | 0.04 |
| **3000** | 14.43 | 0.03 |
| **3500** | 16.74 | 0.05 |
| **4000** | 19.27 | 0.05 |
| **4500** | 21.36 | 0.04 |

was also plastically deformed and pushed towards the borders. This smaller amount of material was then added to the initial shape as negative wear volume. At every new cycle, the negative wear volume might increase or decrease depending on the effect of the abrasion action that can add new material or remove part of the material that had been previously built up on the wear area borders. The different alteration of the wear zone borders can motivate the randomization of the amount of negative wear volume (Table 1).

Similar behaviour was observed in the evolution of the test of the Aluminium specimen, whose wear volumes are reported in Table 2 while the evolution of the worn area is shown in Fig. 14.

When comparing the wear test results for the two materials, although having the same diametral wear of about 0.1 mm, the removed material on the Alumide pin reaches about 15 $mm^3$ after 6000 cycles, whereas the corresponding worn volume of the Aluminium specimen is about 21 $mm^3$ at 4500 cycles. The evolution of the worn area confirms the fastest abrasion of the Aluminium material, whose positive wear area is about 65 $mm^2$ after 4500 cycles, while the corresponding area on the Alumide pin is around 50 $mm^2$. The Alumide material reaches the test limit at 6000 cycles with a worn area of around 53.5 $mm^2$.

The wider extension of the worn area on the Aluminium specimen was also confirmed by the photos in Fig. 15, which consider both specimens at the end of the wear test. This figure shows the state of the Aluminium pin after 4500 cycles in the side (Fig. 15a) and top views (Fig. 15c), but also the Alumide pin after 6000 cycles in the same side (Fig. 15b) and top (Fig. 15d) views. By comparing the condition of the two specimens in the photos, it can be noticed that both depth and width of the worn area are larger for the Aluminium pin.

The evolution of wear and the higher resistance of the Alumide specimen can also be displayed in the graph of Fig. 16, wherein the results of this study were combined with the ones of the literature [16]. As it can be noted from the lines of the graph, the evolution of the wear is similar for both materials up to 2500 cycles. After this number of cycles, the increase in the worn volume for the Alumide material is lower than the one of the Aluminium. In fact, the slope of the orange lines changes after 3000 cycles.

The wear behaviour of the two materials can also be compared to the one of acrylonitrile butadiene styrene (ABS). In a previous work [15], the reverse guillotine was used to apply wear to 3D printed ABS fixtures but at a double sliding speed of 1.20 m/min. The ABS pins reached the test limit of 0.10 mm diametral wear before 3000 cycles, thus it could be estimated that by halving the sliding wear velocity, the durability of ABS doubles. Under this assumption, which should be experimentally verified, the lifetime of the ABS fixture would be shorter than the one of the Alumide material in this study.

## 5. Summary and conclusions

In this paper, a methodology for calculating wear volumes on cylindrical geometries from 3D surface data of the worn zone was defined. The methodology is applied to wear evaluation of 3D printed fixtures of Alumide material. The results are also compared to the one of a similar fixture made of AA2024 Aluminium alloy.

Both fixtures were subjected to a wear test to simulate the material consumption for inspection operations of sheet metal parts. The wear tests were carried out using a customized tribome-

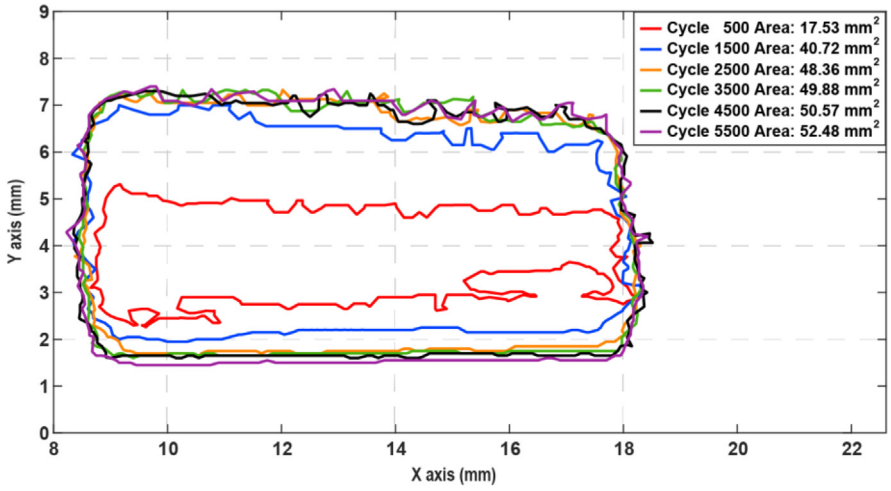


**Fig. 13.** Positive wear area expansion in the top view of XY plane for the Alumide sample at different numbers of wearing cycles.

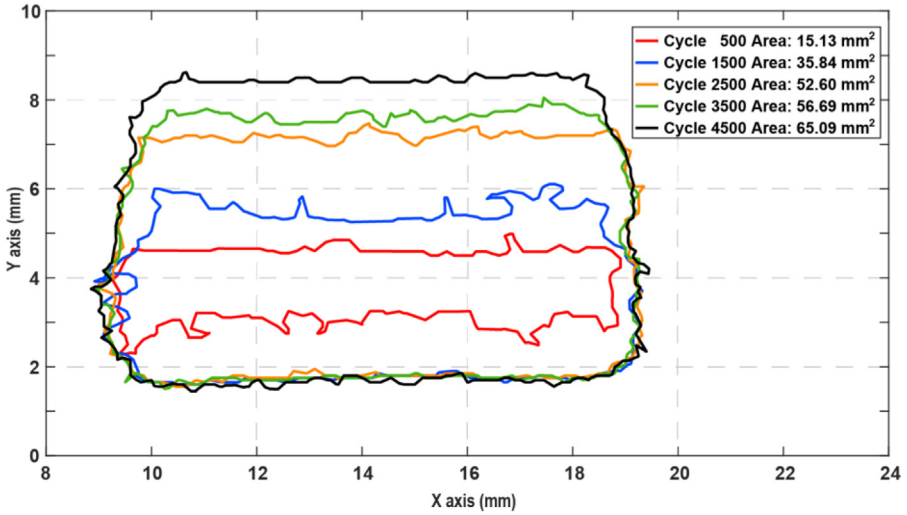


**Fig. 14.** Positive wear area expansion in the top view of XY plane for the Aluminium sample at different numbers of wearing cycles.

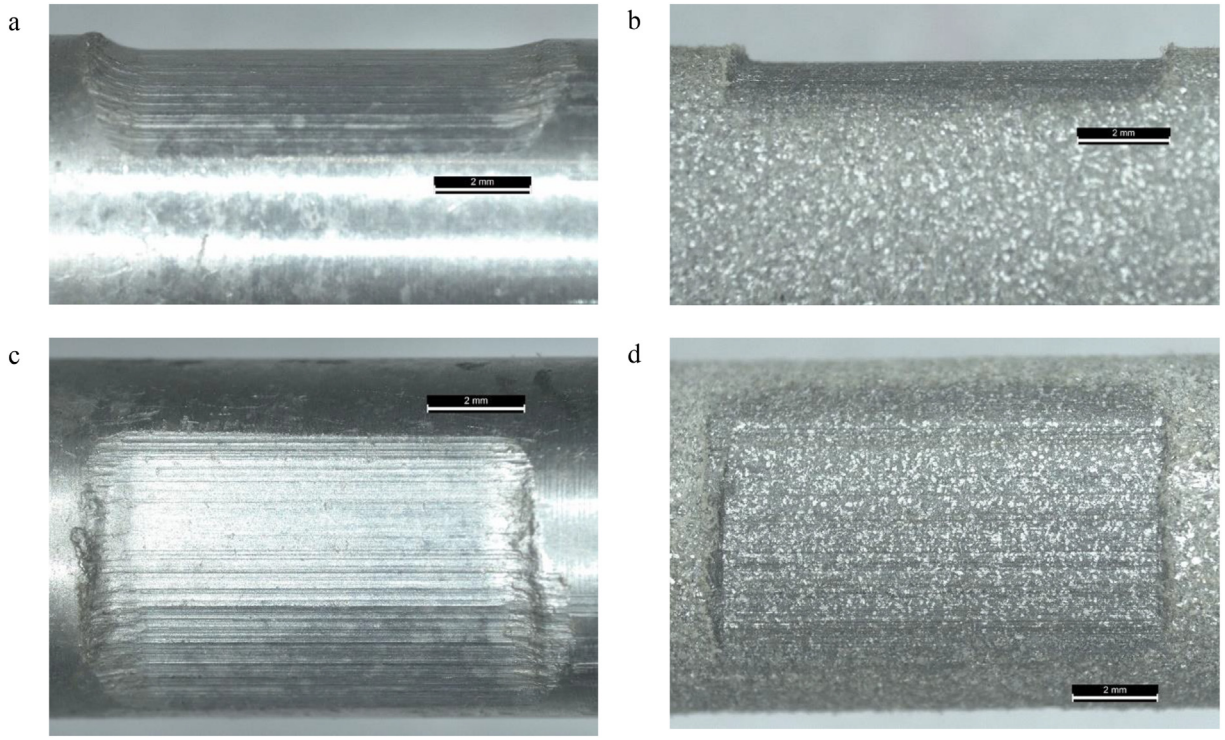


**Fig. 15.** Worn Aluminium pin at 4500 cycles: side view (a) and top view (c); worn Alumide pin at 6000 cycles: side view (b) and top view (d).

ter and the surface condition of the samples was inspected by contact 3D scanning using a Roland Picza Pix-4 device.

Starting from the 3D point cloud data acquired by the Picza scanner, the evaluation procedure differentiates the worn zones and then their 3D volume is generated using alpha shapes. Using the proposed methodology, the value of the worn volumes of the fixture and the extension of the worn zone were evaluated for increasing numbers of wear cycles till reaching an average diametral wear of 0.10 mm for the fixture pin.

The Alumide fixture lasted 6000 cycles with a worn volume of around 15 $mm^3$ on a worn area of 53.5 $mm^2$. The wear resistance of the Aluminium specimen was lower since a worn volume of about 21 $mm^3$ was evaluated for a worn area of around 65 $mm^2$.

Beyond these first results, the wear tests and data analysis should be replicated for a wider number of fixtures to account for material variability and get a wider statistical significance. However, the proposed procedure for estimating wear volumes from 3D scanning surface points is an interesting strategy because it can be applied to a wider range of applications.

## CrediT authorship contribution statement

**Mankirat Singh Khandpur:** Methodology, Investigation, Formal analysis, Visualization, Writing – original draft. **Paolo Minetola:** Conceptualization, Methodology, Investigation, Visualization, Writing – review & editing. **Vito Stiuso:** Formal anal-

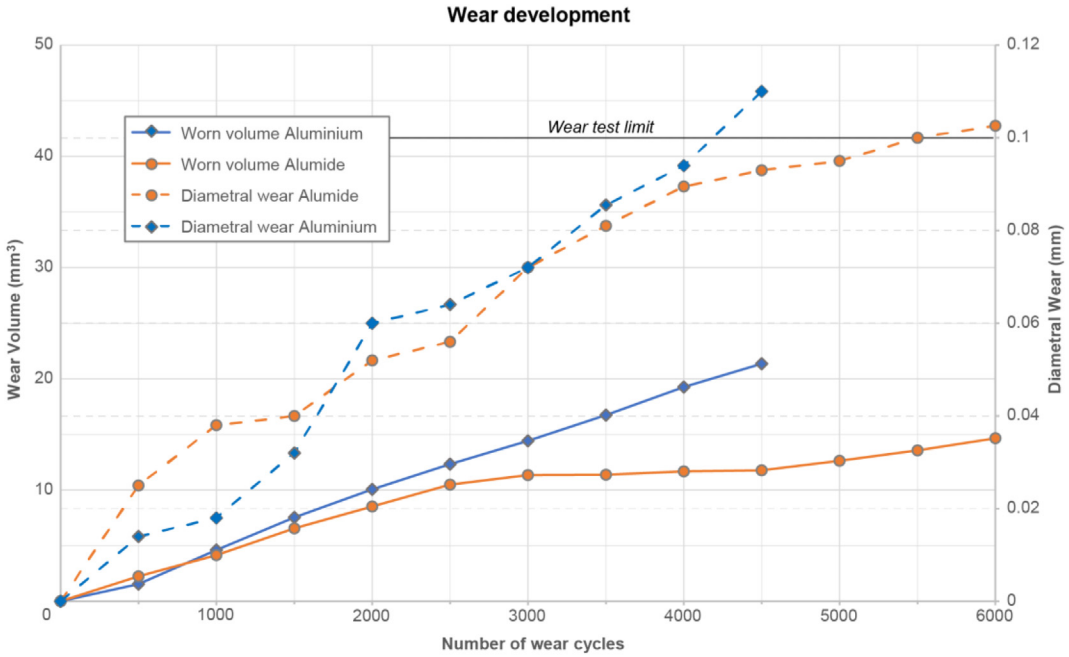


**Fig. 16.** Positive wear at different cycles for the Alumide and Aluminium specimens.

ysis. **Serena Rifuggiato:** Formal analysis. **Luca Fontana:** Data curation. **Erika Lannunziata:** Validation. **Alberto Giubilini:** Data curation, Validation, Writing – review & editing. **Luca Iuliano:** Supervision, Resources.

## Data availability

No data was used for the research described in the article.

## Declaration of Competing Interest

The authors declare that they have no known competing financial interests or personal relationships that could have appeared to influence the work reported in this paper.

## References

[1] A.A. Gameros, D. Axinte, H.R. Siller, S. Lowth, P. Winton, Experimental and numerical study of a fixturing system for complex geometry and low stiffness components, J. Manuf. Sci. E. 139 (045001) (2017) 1–12.
[2] F. Calignano, D. Manfredi, E.P. Ambrosio, S. Biamino, M. Lombardi, E. Atzeni, A. Salmi, P. Minetola, L. Iuliano, P. Fino, Overview on additive manufacturing technologies, Proc. IEEE 105 (4) (2017) 593–612.
[3] A.O. Laplume, B. Petersen, J.M. Pearce, Global value chains from a 3D printing perspective, J. Int. Bus. Stud. 47 (5) (2016) 595–609.
[4] S.B. Mishra, R. Pattnaik, S.S. Mahapatra, Parametric analysis of wear behaviour on fused deposition modelling build parts, Int. J. Product. Qual. Manag. 21 (3) (2017) 375–391.
[5] A. Kampker, G. Bergweiler, A. Ansgar Hollah, A. Lichtenthäler, S. Leimbrink, Design and testing of the different interfaces in a 3D printed welding jig, Proc. CIRP 81 (2019) 45–50.
[6] D.A. Maisano, E. Verna, P. Minetola, V. Lunetto, A.R. Catalano, P.C. Priarone, A structured comparison of decentralized additive manufacturing centers based on quality and sustainability, Int. J. Adv. Manuf. Technol. 121 (2022) 993–1014.
[7] G.M. Violante, L. Iuliano, P. Minetola, Design and production of fixtures for free-form components using selective laser sintering, Rapid Prototyp. J. 13 (1) (2007) 30–37.
[8] G. Schuh, G. Bergweiler, F. Fiedler, K. Lichtenthaler, S. Leimbrink, Hybrid Welding Jigs with Additive Manufactured Functional Elements, in: 2019 IEEE International Conference on Industrial Engineering and Engineering Management (IEEM), 2019, pp. 484–488.
[9] K. Lichtenthaeler, G. Bergweiler, A. Kampker, A. Hollah, S. Leimbrink, Additive Manufacturing for Cost Efficient Hybrid Welding Jigs, in: the 10th International Conference on Engineering, Project, and Production Management EPPM2019, 2020, pp. 559–571.
[10] F. Calignano, M. Lorusso, I. Roppolo, P. Minetola, Investigation of the mechanical properties of a carbon fibre-reinforced nylon filament for 3D printing, Machines 8 (3) (2020) 52.
[11] A. Gameros, S. Lowth, D. Axinte, A. Nagy-Sochacki, O. Craig, H.R. Siller, State-of-the-art in fixture systems for the manufacture and assembly of rigid components: A review, Int. J. Mach. Tool Manu. 123 (2017) 1–21.
[12] N. Krznar, A. Pilipović, M. Šercer, Additive manufacturing of fixture for automated 3D scanning–case study, Procedia Eng. 149 (2016) 197–202.
[13] V. Sindhu, S. Soundarapandian, Additive manufacturing fixture box for bone measurement, Procedia Engineer. 184 (2017) 1–9.
[14] P. Jagadeesh, M. Puttegowda, Y.G.T. Girijappa, S.M. Rangappa, M.K. Gupta, S. Siengchin, Mechanical, electrical and thermal behaviour of additively manufactured thermoplastic composites for high performance applications, in: Additive and Subtractive Manufacturing of Composites, Springer, 2021, pp. 167–199.
[15] P. Minetola, L. Iuliano, Investigation of wear behaviour of FDM fixtures, in: Innovative Developments in Virtual and Physical Prototyping, CRC Press, 2012, pp. 749–756.
[16] P. Minetola, L. Iuliano, The reverse guillotine tribometer for evaluation of sliding wear of additive manufactured fixtures, Rapid Prototyp. J. 20 (2) (2014) 105–114.
[17] P. Minetola, L. Iuliano, F. Calignano, A customer oriented methodology for reverse engineering software selection in the computer aided inspection scenario, Comput. Ind. 67 (2015) 54–71.